Archive of SID.ir

Journal of Petroleum Science and Technology 12(1): 33, 2022, Pages 42-51
DOI:10.22078/JPST.2022.4848.1810

Journal of Petroleum Science and Technology
Research Paper
https://jpst.ripi.ir/

# AVO Analysis of Bottom Simulating Reflector (BSR) for Hybrid Model of Gas Hydrate Distribution

**Hoda Yari[1], Majid Nabi Bidhendi[2]*, Nasser Keshavarz Farajkhah[3] and Reza Heidari[1]**

*1. Department of Earth Sciences, Science and Research Branch, Islamic Azad University, Tehran, Iran*
*2. Institute of Geophysics, University of Tehran, Iran*
*3. Geoscience Faculty, Research Institute of Petroleum Industry (RIPI), Tehran, Iran*

## Abstract

Due to the substantial effect of the gas hydrate distribution model (cement, un-cement, or hybrid of both models) on the elastic properties (such as shear modulus, bulk modulus, Poisson's ratio, etc.), determining the distribution model in the hydrate-bearing sediments is a requirement for decreasing uncertainty in quantitative studies based on seismic velocities. Many different empirical and theoretical rock physics theories cover different ranges of rock properties. Among them, the Effective Medium Theory (EMT) is the most appropriate in quantitative studies of gas hydrate resources. Four types of hydrate distributions have been considered and divided into two cemented and un-cemented categories. EMT is one of the advanced rock physics modeling tools. This theory has been modified by introducing hybrid distribution models of gas hydrate instead of having assumptions about single models of hydrate distribution. Moreover, when a scientific manuscript is written, using dangling and misplaced modifiers are not suggested. On the other hand, one method to determine the gas hydrate distribution model can be performed by identifying AVO's class on the bottom simulating reflector (BSR); caused by the contrast between an overlying gas hydrate and underlying free gas sediments. This reflector mimics seafloor topography, cross-cuts stratigraphic reflections, and is controlled by thermodynamic conditions. The results of this study on conceptual models showed that in hybrid approach for hydrate distribution, AVO's class on BSR shows sensitivity to (1) the combination type of gas hydrate distributions models, (2) the total saturation of the gas hydrate and free-gas across the BSR.

***Keywords:*** Gas Hydrate Distribution, Effective Medium Theory (EMT), Hybrid Models, Amplitude Variation vs Offset (AVO).

## Introduction

This study is based on effective medium theory; in this theory, four models of gas hydrate distribution have been considered. In the first model, it is assumed that the gas hydrate is suspended in the water, and it only participates in the compression modulus of the pore water, and there was no contact surface between the sediment and the gas hydrate, which this model is called non-contact. This study is based on effective medium theory; in this theory, four models of gas hydrate distribution have been considered. In the first model, it is assumed that the gas hydrate is suspended in the water, and it only participates in the compression modulus of the pore water, and there was no contact surface between the sediment and the gas hydrate, which this model is called non-contact. The second model was one of the non-contact models; moreover, the gas hydrates was attached to the solid particles, but it didn't have any effects on the cementation.

In the third model, gas hydrates have acted at the contact site of the particle, such as cement. Finally, in the fourth model, a sediment particle is coated by a gas hydrate, reducing the porosity and increasing the sediment rigidity.

Each of the four gas hydrate distribution models is utilized to predict the elastic properties of the environment exclusively based on EMT. For example, gas hydrates saturated cementation models affect the rock's shear and compression modulus and increase it. Whereas non-cementation models do not have much effect on the shear modulus of the rock and it only affect the compression modulus.

Also, each gas hydrate distribution model predicts the elastic properties based on their physics.

**Corresponding author:* Institutes of Geophysics, University of Tehran, Iran
*E-mail addresses: mnbhendi@ut.ac.ir*
*Received 2022-06-30, Received in revised form 2022-08-12, Accepted 2022-10-18, Available online 2022-12-13*

Archive of SID.ir

Archive of SID.ir



For example, cementation models have a large effect on the shear and compression modulus of the rock and significantly increase them, whereas non-cementation models have only effects on s compression modulus.

The variation rate in shear wave velocity depends on the type of gas hydrate distribution. For example, the rate of shear wave velocity increased dramatically with the presence of gas hydrates inside the porosity. However, if the gas hydrate only occupies the porous space and suspends in water, it has a minimal increase in shear wave velocity. Presence of free gas in the host sediment decreases bulk modulus, and it doesn't change shear modulus, and as a consequence, free gas causes drop in compressional velocity, and it slightly increases shear velocity since the density is decreased.

Analysis of amplitude versus offset variation is used as an effective method for determining reservoir characteristics [1]. The success of this method depends on various factors, such as the quality of recorded information, the processing of seismic data, and the correct understanding of the rock's physical characteristics.

Incidence the compression wave to the common boundary of two layers with different elastic characteristics causes two types of energy: (1) some of the energy reflected as (a) compression and (b) shear waves and (2) some of the energy passes.

By establishing boundary conditions (continuity of stress and displacement at the common boundary of two layers), Zoeppritz provided the possibility of calculating the reflected wave amplitude and wave amplitude passing through the common boundary condition [2].

It also calculated the reflection amplitude and passing amplitude values for two compression and shear waves. However, it is not easy to investigate and analyze the effective quantity in the behavior of AVO using the Zoeppritz relationship due to the non-linear and multiplicity of elastic quantity in the equation.

Several equations have been presented In order to investigate the factors affecting AVO, several equations have been presented. The Aki, Richards [3] and Wiggins [4] equations are utilized.The purpose of the inversion of AVO in pre-stack seismic data is to obtain the coefficients of Zoeppritz's linearized equations.

Different classes for the common boundary of a sandstone layer containing gas and a layer on it have been expressed by Rutherford and Williams [5], in which the determinant factor is the reflection coefficient in vertical wave incidence (R0) mode.

In the first class of AVO, the reflection coefficient at the common boundary in the zero-offset is positive, and it decreases by increasing offset. In the second class of AVO, the reflection coefficient is minor and near zero, which moves toward negative values by increasing offset. In the third class of AVO, the reflection coefficient is negative, and when the offset is increased, the absolute value of amplitude increases. Therefore, variations in AVO responses can be directly related to Poisson's ratio variations, which it is an indicator of fluid changes.

For example, in the case of gas hydrate sources, when there is some free gas inside the sub-bottom sediments of gas hydrates, the compression wave velocity decreases greatly; however, the shear wave velocity increases a bit due to the reduction of density. The decrease in the compression wave velocity causes changes in the reflection coefficient, a reduction in VP/VS ratio, and a severe decline in Poisson's ratio, which ultimately leads to an increase in amplitude versus offset [6] and the third class of AVO can be considered for it. As shown in Figure 1, Castagna [7] called the classification by Rutherford and Williams unfinished and introduced the fourth class of AVO. In this class, the reflection coefficient in the common boundary is negative, but by increasing the offset, the amplitude value increases algebraically and decreases in the absolute value of amplitude.

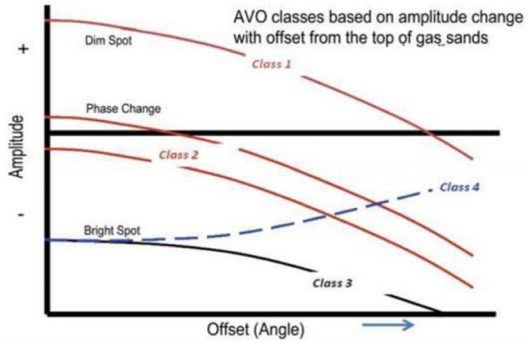


**Fig. 1** Amplitude versus offset variation for four AVO classes [5].

Several researchers have used the AVO method to conduct qualitative studies of gas hydrate sources [8, 9]. AVO method alone or in combination with other methods has been used for few studies [10-12]. Rock physics inversions in which elastic properties are related to the saturation of hydrates and free gas, so studying gas hydrate sources using quantities methods is important; therefore, in this issue, several researchers have been investigated [13]. Gas hydrate and free gas can cause apparent AVO anomalies and reveal various seismic indicators of gas hydrate and free gas [14]. AVO analysis and seismic inversion to examine detailed properties from the BSR are conducted [15]. Four different gas hydrate and free gas configurations were simulated through AVO forward modeling. The results showed that the AVO attribute characteristics were sensitive for identifying gas hydrate but significantly affected by free gas [16]; because only a small percent of free gas below BSR can significantly change Poisson's ratio of underlying sediment. In previous studies, the BSR at the seismic section has been used as the main indication for determining the presence range of gas hydrate in the Oman Sea [17], and AVO analysis for the BSR was based on only one gas hydrate distribution model [18, 19]. In this study, AVO analysis of BSR for a combined gas hydrate distribution model has been investigated.

One of the effective factors on elastic properties is the type of gas hydrate distribution in the host sediment. There are different classifications for rock physic models of gas hydrate, and among them, the most important and most applicable one is the classification introduced by Ecker [20]. This classification considers four different models for how gas hydrates are distributed within sediment porosity. In the first model, gas hydrate is suspended in water, with no contact surface between sediments and gas hydrates, and called non-contact.

Archive of SID.ir

Archive of SID.ir



In the second model, one of the contact models, gas hydrates are attached to solid particles but have no effect on sediment cementation; therefore, the first and second models are named non-cementing models.

In the third model, gas hydrates act as cement at the contact between the particles, causing more sediment consolidation. In the fourth model, the hydrate covers entire of the sediment particles and reduces porosity and also increases sediment strength. Therefore, the third and fourth models named as cementing models. The variation rate in shear wave velocity depends on the type of gas hydrate distribution. This rate increases dramatically with the presence of gas hydrates saturation inside the porosity. Different hybrid distributions of gas hydrate have been investigated in this article. Velocity waves of single distribution of second and third models and combination of second and third distribution models are shown in Figure 2.

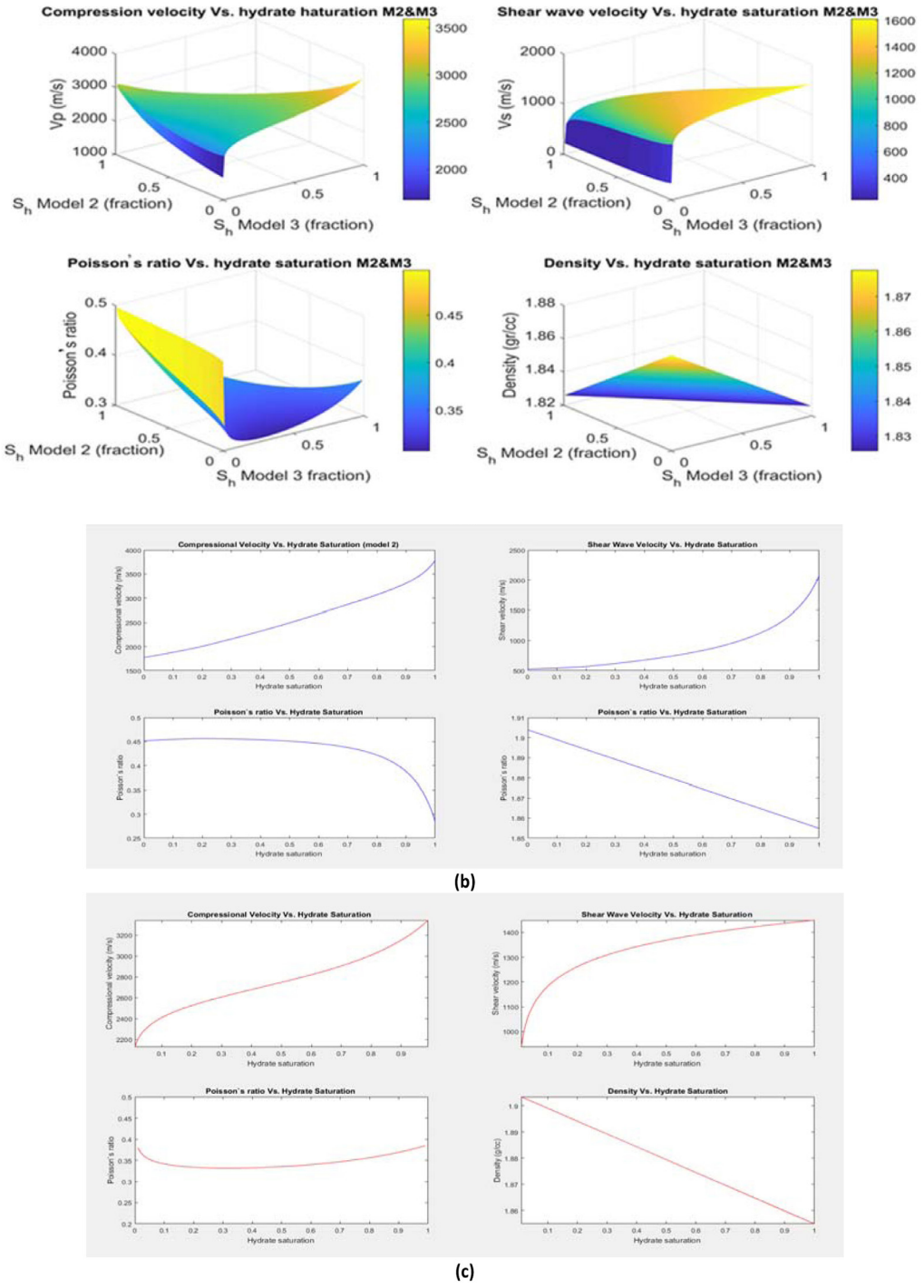


**Fig. 2** The results of estimating the compression wave velocity, shear wave velocity, density and Poisson's ratios for different percentages of gas hydrate saturation. (a) Hybrid distribution of Model 2 and 3 (b) single Model of second distribution, and (c) single Model of third distribution, [21].

Archive of SID.ir

Archive of SID.ir



The elastic properties that considered for hybrid modeling of gas hydrate distribution based on (EMT) are shown in Table 1. Sedimentological properties, which used for modeling rock physics including mineralogical composition, gas hydrate and free gas saturations, critical porosity and etc. are shown in Table 2.

**Table 1** Elastic properties of different constituents for rock physics modeling [22].

| Components | Bulk modulus (GPa) | Shear modulus (GPa) | Density (g/cm$^3$) | P-wave velocity (m/s) | S-wave velocity (m/s) |
|---|---|---|---|---|---|
| Clay | 20.9 | 6.85 | 2.58 | 3412 | 1629 |
| Quartz | 36 | 45 | 2.65 | 6018 | 4121 |
| Hydrate | 6.41 | 2.54 | 0.91 | 3281 | 1670 |
| Sea water | 2.49 | 0 | 1.03 | 1554 | 0 |
| Gas (methane) | 0.11 | 0 | 0.23 | 691 | 0 |

**Table 2** Parameters used for conceptual modeling.

| | Parameters | Values |
|---|---|---|
| Sedimentological | Quartz percent | 40% |
| | Clay percent | 60% |
| | Average grain contact number, n | 8 |
| | Sediment porosity | ~50% |
| | Critical porosity, $\phi_0$ | 40% |
| | Gas hydrate saturation | (0-25)% |
| | Free gas saturation | 10% |
| Geometrical | Seafloor depth | 1280 m |
| | Top of hydrate depth | 1400 m |
| | BSR depth | 1650 m |
| | BGR (Bottom of Gas Reflector)depth | 1700 m |

Non-cementing models show (first and second models) the second or third classes of AVO, and cementing models (third and fourth models) show the fourth class of AVO for the usual saturations [18]. In this research, hybrid gas hydrate distribution models [21] (a combination of cement and non-cement models) are considered to investigate and analyze the AVO behavior of BSR as conceptual models.

## Modeling Synthetic Data Containing Gas and Free Gas Hydrates

In this study, a simple model containing five layers has been considered: (1) water column, (2) layer of fully water saturation, (3) gas hydrate-bearing layer, (4) layer containing free gas, and (5) fully saturated sediment with water. Compression and shear wave velocities of sediments for these layers including hybrid distribution models have been calculated based on effective medium theory by developing script in MATLAB, as shown in Figure 3.

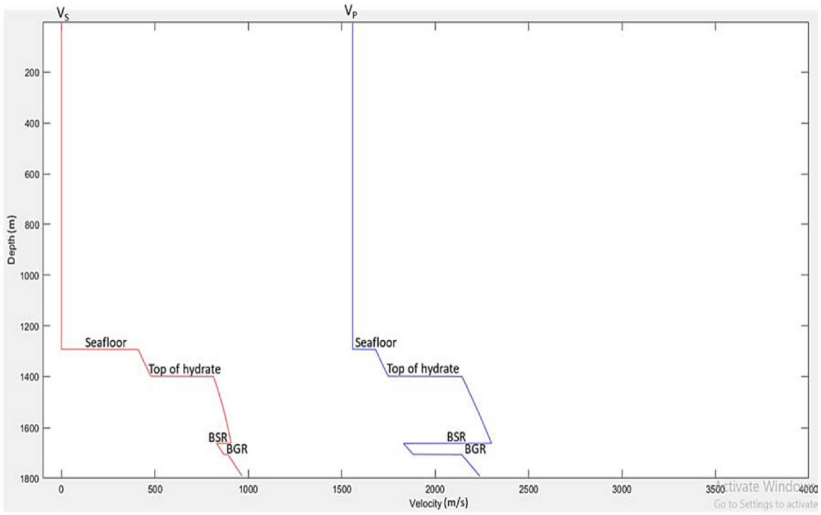


**Fig. 3** Compression and shear wave velocity-depth modeled based on the hybrid distribution of the second and fourth gas hydrate models in MATLAB software.

Archive of SID.ir

Archive of SID.ir



Various ranges of gas hydrate saturation were considered for constructing the synthetic model. Thus, the elastic parameters of all layers were calculated. Then, forward modeling for synthetic traces was performed using a wave equation modeling algorithm to investigate their seismic response in Hampson Russell software, and common middle point records were generated.

In the following, as shown in Figure 4 to 13, the results of AVO analyses using Wiggin's equation on BSR for synthetic traces are explained.

$$R(\theta) = A + B\sin^2\theta + C\tan^2\theta\sin^2\theta \quad (1)$$

The equation (Equation 1) was separated into three reflection terms by Wiggin, which it is expressed as follows:

$$A = \frac{1}{2}\left[\frac{\Delta V_P}{V_p} + \frac{\Delta\rho}{\rho}\right] \quad (2)$$

$$B = \frac{1}{2}\frac{\Delta V_P}{V_p} - 4\left[\frac{V_S}{V_P}\right]^2\frac{\Delta V_S}{V_S} - 2\left[\frac{V_S}{V_P}\right]^2\frac{\Delta\rho}{\rho}$$

$$C = \frac{1}{2}\frac{\Delta V_P}{V_p}$$

For instance, a combination of the second and fourth models of distribution for gas hydrate with saturations of 10% and 20%, respectively for the second and fourth models is shown in Figure 4. It also shows synthetic trace, density, compression, and shear wave velocities logs. In Table 3, the parameters, which are required for synthetic seismogram and AVO analyses, are shown.

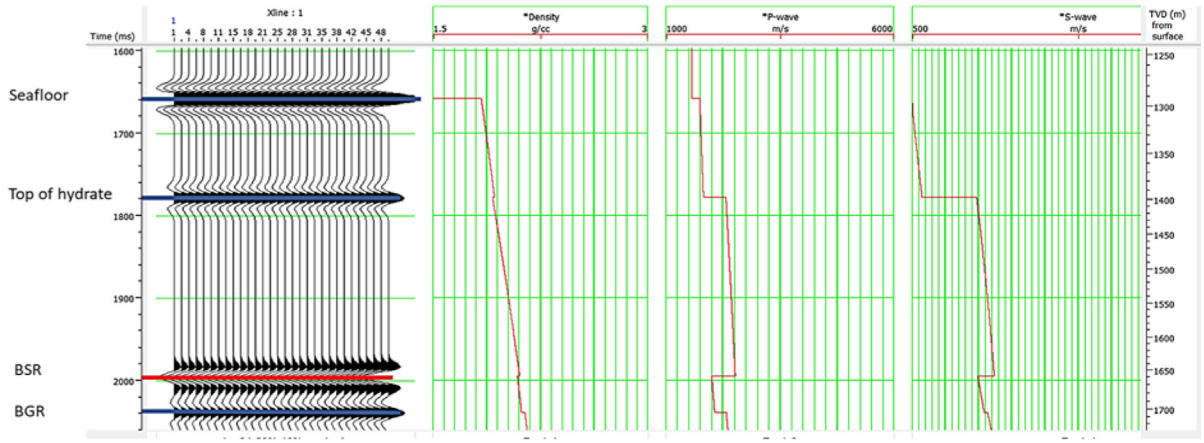


**Fig. 4** Synthetic data based on the hybrid distribution of the second and fourth gas hydrate models.

**Table 3** Parameters intended to obtain seismic response and AVO analyses.

| Geometry of source and receivers | Intended Parameters |
|---|---|
| Wavelet | Ricker wavelet With a dominant frequency of 30 Hz |
| Number of receivers | 120 |
| Offset area | 6120-120 m |
| Sample rate | 2ms |
| Type of forward modeling | Wiggin's equation |

In combination of the second and the fourth distributions of gas hydrate; the second distribution with 10% of gas hydrate saturation and the fourth distribution of gas hydrate by three ranges (5%, 15% and 20%) of gas hydrate saturations have been considered.

AVO variation on the BSR for the second distribution of gas hydrate and the fourth distribution of gas hydrate containing 5% of gas hydrate saturation is shown in Figure 5.

AVO variation on the BSR for the second distribution of gas hydrate and the fourth distribution of gas hydrate containing 15% of gas hydrate saturation is shown in Figure 6.

AVO variation on the BSR for the second distribution of gas hydrate and the fourth distribution of gas hydrate containing 20% of gas hydrate saturation is shown in Figure 7.

In combination of the first and the fourth distributions of gas hydrate, the first distribution with 10% and three ranges (5%, 10% and 15%) of gas hydrate saturation for the fourth distribution of gas hydrate have been considered. AVO variation on the BSR for the second distribution of gas hydrate and the fourth distribution of gas hydrate containing 5% of gas hydrate saturation is shown in Figure 8.

AVO variation on the BSR for the second distribution of gas hydrate and the fourth distribution of gas hydrate containing 10% of gas hydrate saturation is shown in Figure 9.

AVO variation on the BSR for the second distribution of gas hydrate and the fourth distribution of gas hydrate containing 15% of gas hydrate saturation is shown in Figure 10.

In Figures 11 and 12, AVO behavior for combining of non-cement models with 15% of gas hydrate saturation and third distribution of gas hydrate with 5% of gas hydrate saturation is shown.

The combination of non-cementing model with 10% of gas hydrate saturation for the first distribution of gas hydrate and 15% of gas hydrate saturation for the second distribution of gas hydrate is shown in Figure 13.

Archive of SID.ir

Archive of SID.ir



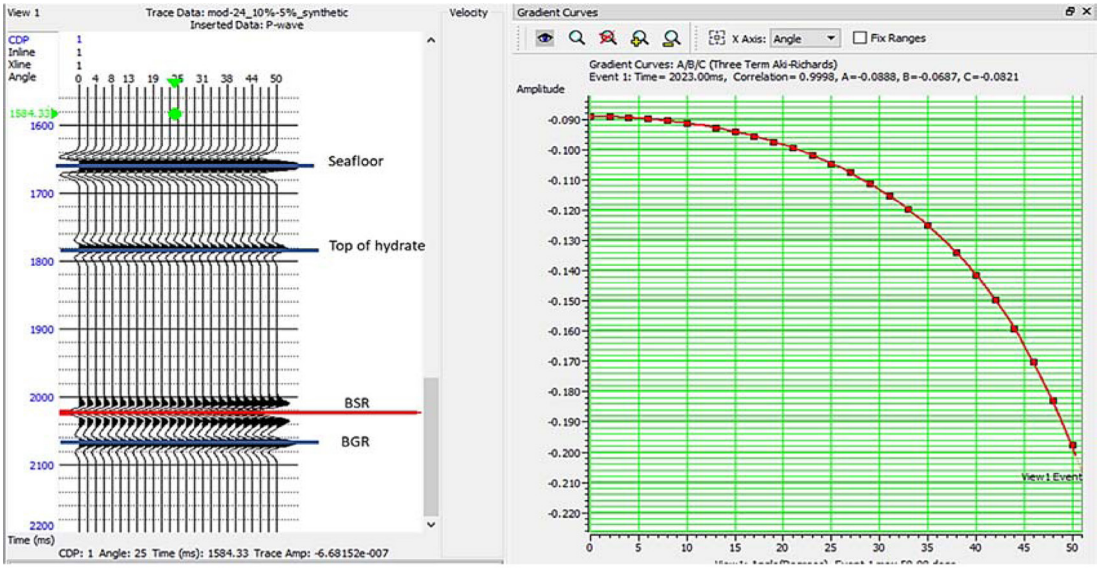


**Fig. 5** The hybrid distribution of the second model with 10% and the fourth model with 5% saturation for gas hydrate results from the third class of AVO.

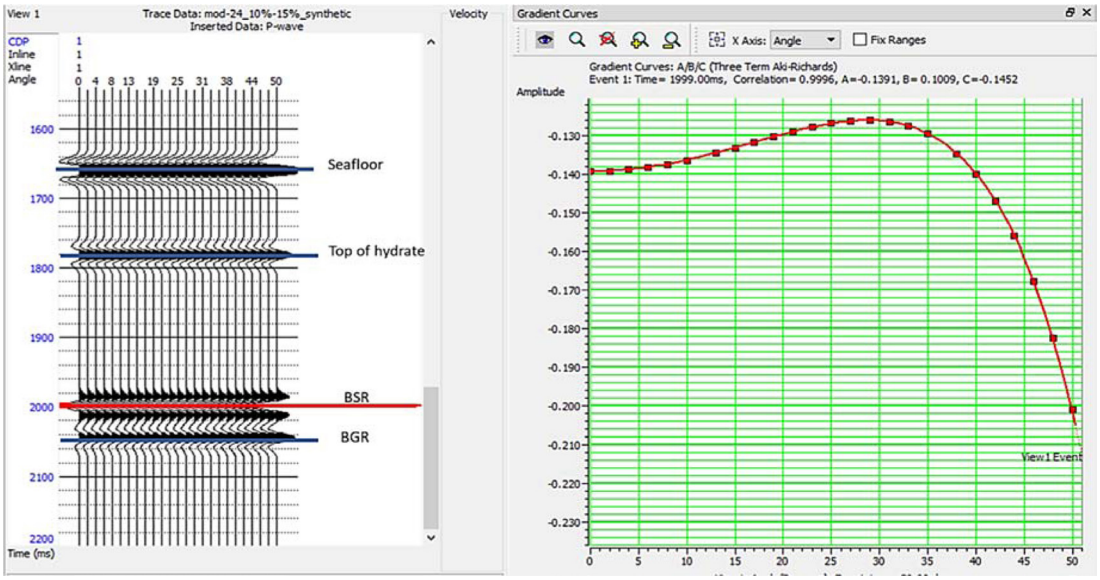


**Fig. 6** The hybrid distribution of the second model with 10% and the fourth model with 15% of gas hydrate saturation results from the fourth class of AVO.

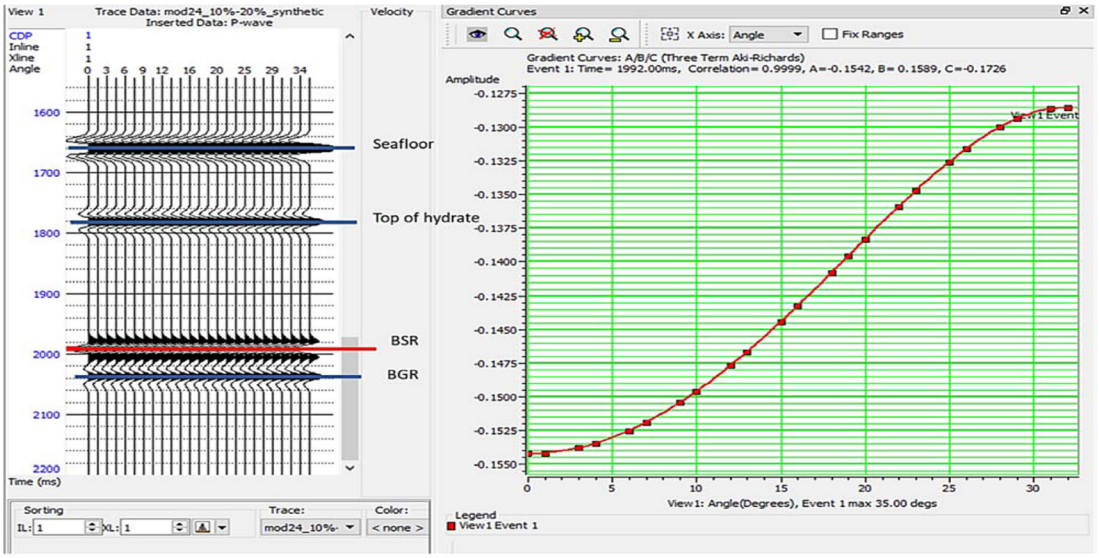


**Fig. 7** The hybrid distribution of the second model with 10% and the fourth model with 20% of saturations for gas hydrate with the result of the fourth class of AVO.

Archive of SID.ir

Archive of SID.ir



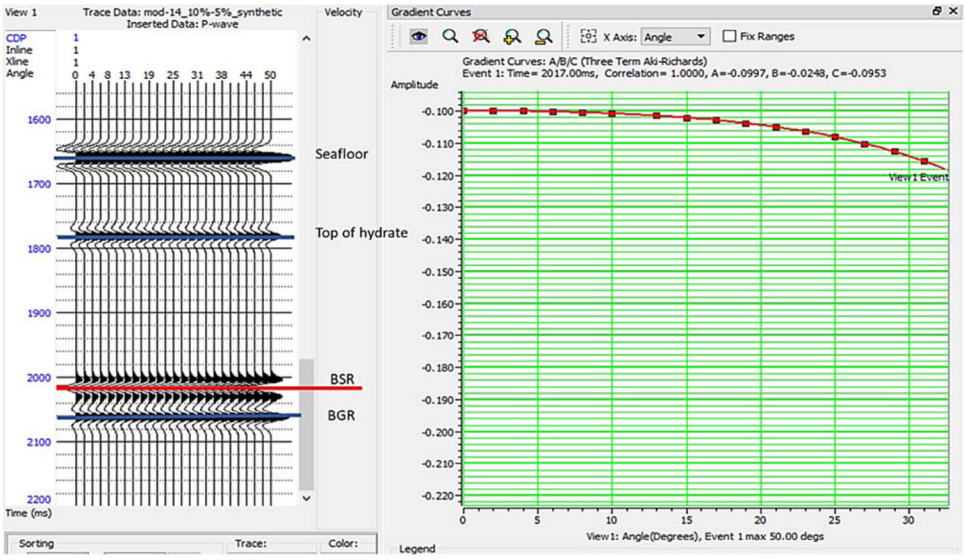


**Fig. 8** The hybrid distribution of the first model with 10% and the fourth model with 5% of saturation for gas hydrate with the result of the third class of AVO.

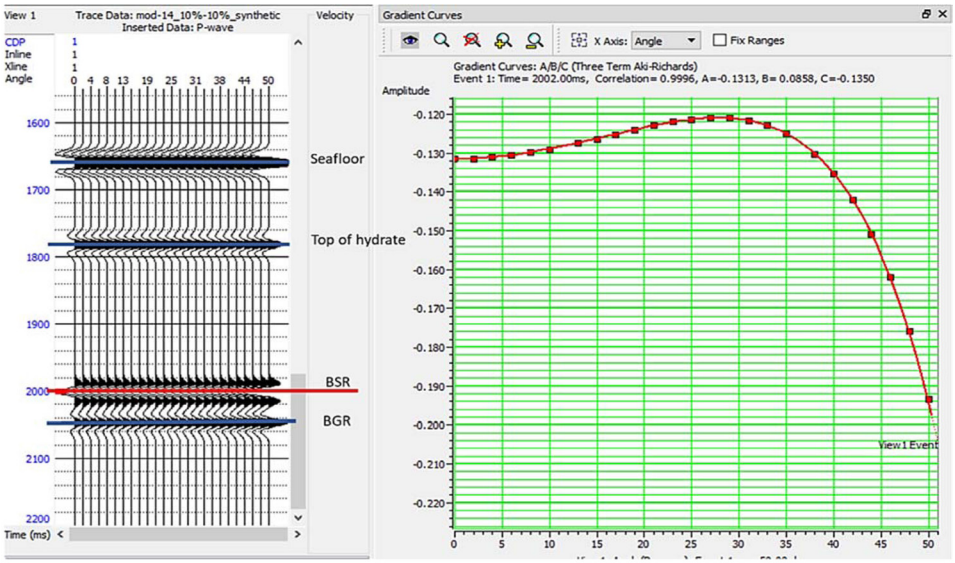


**Fig. 9** The hybrid distribution of the first model with 10% and the fourth model with 10% of saturation for gas hydrate with the result of the fourth class of AVO.

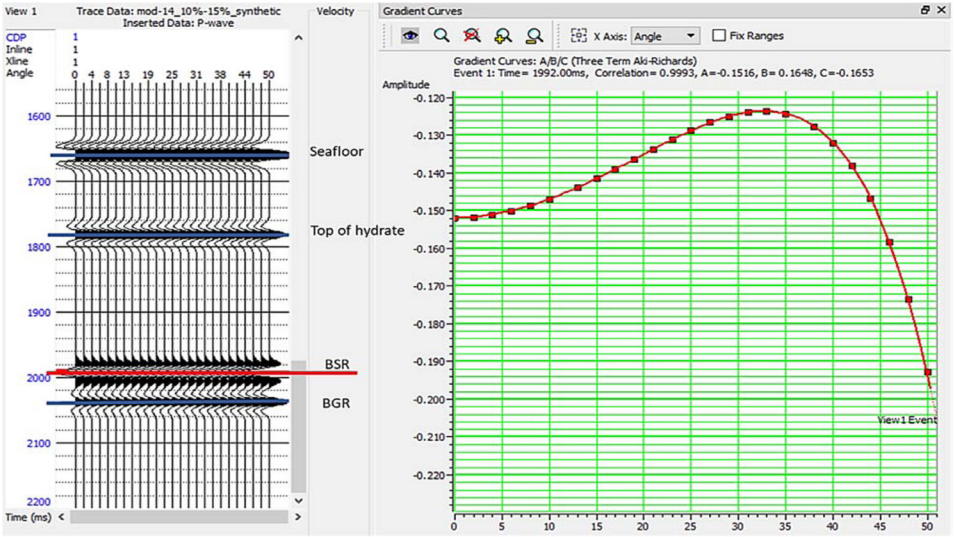


**Fig. 10** The hybrid distribution of the first model with 10% and the fourth model with 15% of saturation for gas hydrate with the result of the fourth class of AVO.

Archive of SID.ir

Archive of SID.ir



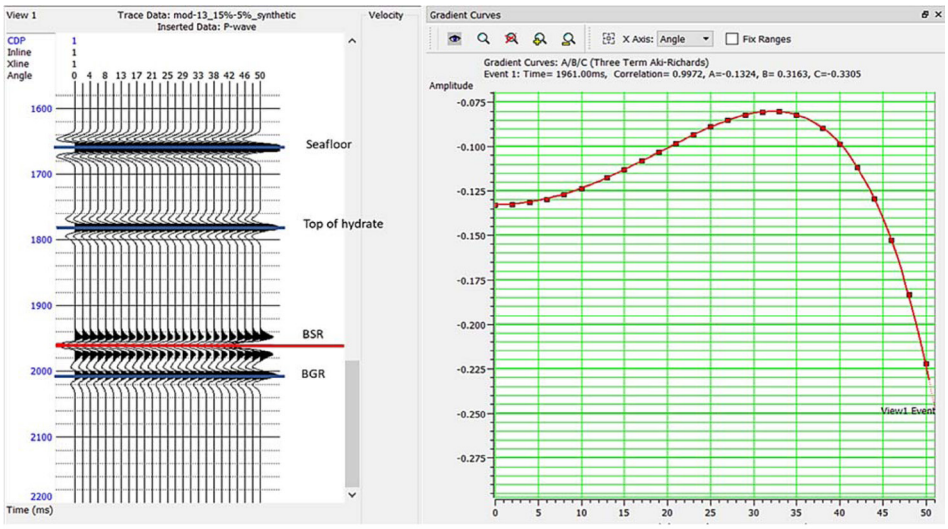


**Fig. 11** The hybrid distribution of the first model with 15% and the third model with 5% of saturation for gas hydrate results from the fourth class of AVO.

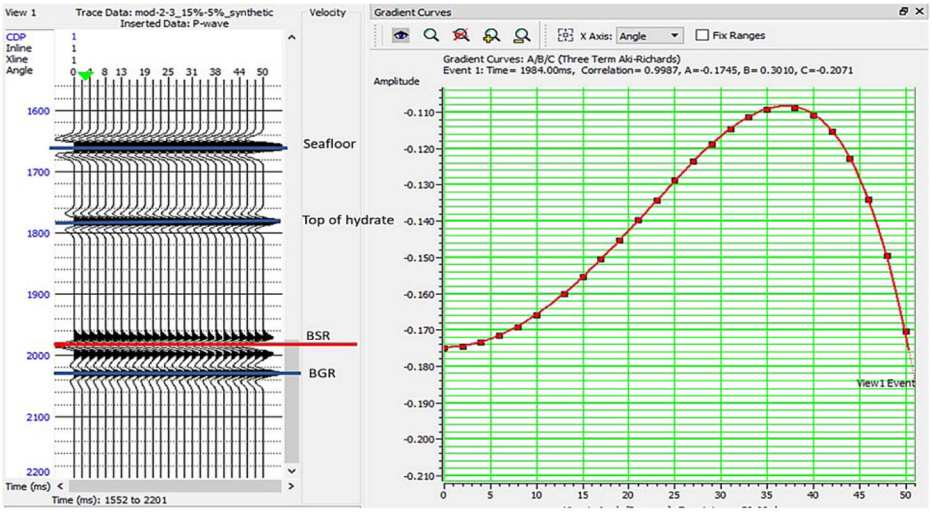


**Fig. 12** The hybrid distribution of the second model with 15% and the third model with 5% of saturation for gas hydrate results from the fourth class of AVO.

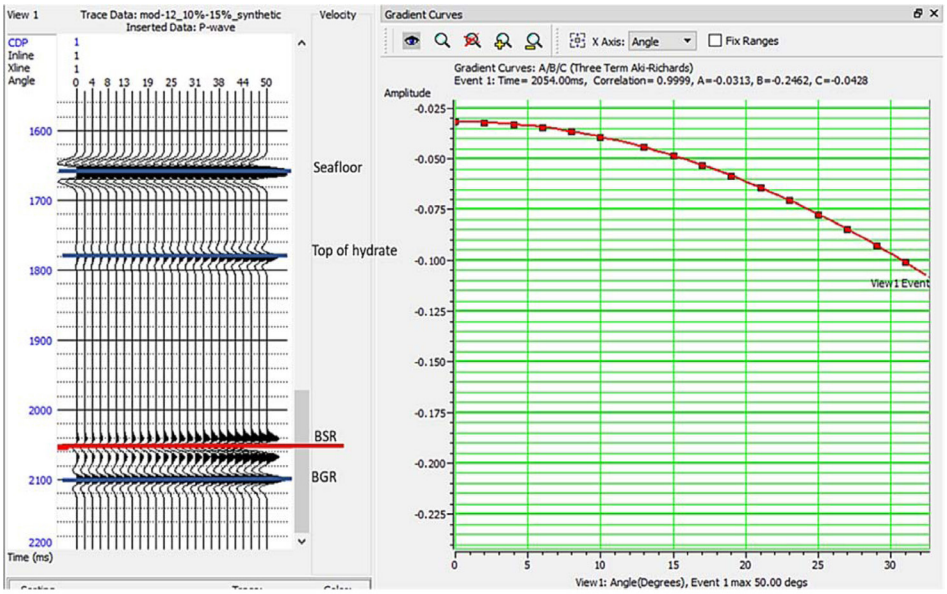


**Fig. 13** The hybrid distribution of the first model with 10% and the second model with 15% saturation for gas hydrate results from the second class of AVO.

Archive of SID.ir

Archive of SID.ir



For evaluation of conceptual modeling performed in this study, the AVO responses for real data have been evaluated and compared with the template generated based on the synthetic modeling. Furthermore, obvious BSR show the presence of hydrate in Iranian part of deep sea of Iran [17]. "The area has been covered by 2-D seismic lines oriented from north to south and from west to east." demonstrates and expresses that your study is really excellent. AVO was analyzed on the different CDP of the one seismic line in this area.

In Figure 14, the seismic section with BSR is shown; furthermore, AVO analyzed for nominated locations A, B and C have been performed. It is observed that the two gathers (locations B and C) show the AVO class IV. Whereas, one gather (location A) shows the AVO class III. They reveal the combination of the cementing and non-cementing effect of the hydrate distributions. The AVO class III shows combination the first (or second) and the fourth distribution models, it depends on the amount of gas hydrate saturation. And thereby, surely, the third gas hydrate distribution model doesn't presence. The AVO class IV in this section shows the combination of the third (or fourth) and the second distribution models.

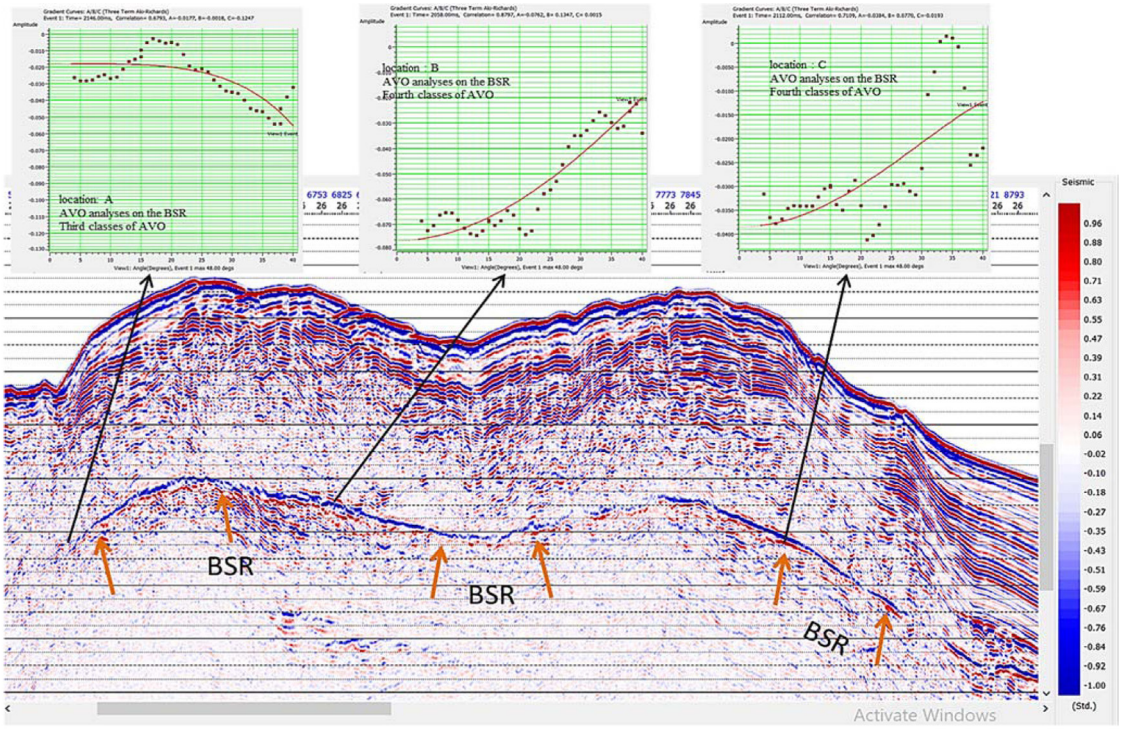


**Fig. 14** AVO analyses on the BSR.

Qualitative analysis using the AVO method for the BSR will help to identify the gas hydrate distribution model and free gas on seismic data. AVO analysis for the BSR helps to identify the gas hydrate distribution model, and consequently, it reduces the uncertainty associated with reservoir properties estimation using rock physics inversion.

## Conclusions

The results of the conceptual model analysis show that the initial guess about possible distribution in hybrid models can be obtained from AVO analysis of BSR. The following conclusions were reached:

1. In the first and second models of gas hydrate distribution (non-cement models), for both hybrid or single distribution cases, the BSRs show the second or third class of AVO depending on the range of gas hydrate and free gas saturations. On the other hand, the greatest variation in elastic properties and AVO behavior of BSR occurs when the hybrid models are obtained from combining the non-cemented models with cement ones.
2. In BSR, AVO classes IV are observed in a hybrid combination composed of the first and fourth models when the saturation of the hydrate distributed as the fourth model is greater than 5%, independent of the saturation value for the first model.
3. In combination with the second and the fourth distribution models, the AVO class is observed when the saturation of the hydrate distributed in the fourth model is greater than 15%, independent of the saturation value for the second model.
4. In the case of combining the third gas hydrate distribution model with non-cementing models, AVO class IV is always observed for all values of the saturations due to the significant effect of the third hydrate distribution model on elastic properties.
5. Ultimately, it can be concluded that the BSR's AVO behaviors depend on the range of the gas hydrate saturation and non-cementing models are less effective than cementing ones. Accordingly, the observation of class AVO IV in BSR can be related to the presence of both cementing and non-cementing models of gas hydrate distribution. Therefore, to have a more accurate quantitative analysis and understanding of hydrate distribution models, it is necessary to implement hybrid distribution models after having an initial guess about probable distributions combined in hybrid models.

Archive of SID.ir

Archive of SID.ir



**Nomenclatures**

BSR: Bottom Simulating Reflector
EMT: Effective Medium Theory
AVO: Amplitude Variation Vs Offset

**References**

1. Khadem B, Javaherian A, (2019) Amplitude variation with offset inversion analysis in one of the western oilfields of the Persian Gulf: Iranian, Journal of Oil and Gas Science and Technology, 8, 2: 15-33.
2. Zoeppritz K (1919) On the reflection and penetration of seismic waves through unstable layers: Erdbebenwellen VIIIB, Goettinger Nachrichten, 1: 66–84.
3. Aki K, Richards P G (1980) Quantitative seismology; theory and methods, W. H. Freeman and Company, 703.
4. Wiggins R, Kenny G S, McClure C D (1983) A method for determining and displaying the shear-velocity reflectivities of a geologic formation, European Patent Application, 0113944.
5. Rutherford SR, Williams RH (1989) Amplitude-versus-offset variations in gas sands, Geophysics, 54: 680–688.
6. Muller C, Bonnemann C, Neben S (2007) AVO study of a gas hydrate deposit; offshore Costa Rica: Geophysical Prospecting, 55: 1–17.
7. Castagna J P, Swan H W, Foster D J (1998) Framework for AVO gradient and intercept interpretation, Geophysics, 63: 948–956.
8. Bo Y Y, Lee G H, Horozal S, Yoo D G, Ryu B J, Kang N K, Kim H J (2011) Qualitative assessment of gas hydrate and gas concentrations from the AVO characteristics of the BSR in the Ulleung Basin, East Sea (Japan Sea), Marine and Petroleum Geology, 28, 10: 1953-1966.
9. Fohrmann M, Pecher I A (2012) Analyzing sand-dominated channel systems for potential gas-hydrate-reservoirs using an AVO seismic inversion technique on the Southern Hikurangi Margin, New Zealand, Marine and Petroleum Geology, 38: 19–34.
10. Ojha M, Sain K (2007) Seismic velocities and quantification of gas-hydrates from AVA modeling in the western continental margin of India, Marine Geophysical Research, 28: 101–107.
11. Ojha M, Sain K (2008) Appraisal of gas-hydrates/free-gas from VP/VS ratio in the Makran accretionary prism, Marine and Petroleum Geology, 25: 637–644.
12. Lu S, McMechan G A (2004) Elastic impedance inversion of multichannel seismic data from unconsolidated sediments containing gas hydrate and free gas, Geophysics, 69: 164-179.
13. Ecker C (1997) Characterization of a hydrate reservoir: Stanford Exploration Project Report, 94: 1-16.
14. Wang X, Pan D (2017) Application of AVO attribute inversion technology to gas hydrate identification in the Shenhu Area, South China Sea, Marine and Petroleum Geology, 80: 23-31.
15. Choi Y, Kang S G, Jang U G, Kuk Hong J, Jin Y K, Keen Chung W, Shin S R (2018) AVO analysis to gas hydrates BSR in the continental shelf of canadian beaufort sea, In EGU General Assembly Conference Abstracts, 13844.
16. Zhang X, Yin C, Zhang G (2021) Confirmation of AVO attribute inversion methods for gas hydrate characteristics using drilling results from the shenhu area, South China Sea, Pure Appl Geophys, 178: 477–490.
17. Shoar B H (2008) Identification of gas hydrate sediments in the Oman Sea and their seismic survey, Faculty of Mining Engineering, Metallurgy and Petroleum of Amirkabir University of Technology: Master Thesis.
18. Shoar B H, Javaherian A, Farajkhah N K, Arabani M S (2014) Reflectivity template, a quantitative intercept-gradient AVO analysis to study gas hydrate resources–A case study of Iranian deep-sea sediments, Marine and Petroleum Geology, 51: 184-196.
19. Salehi E, Javaherian A, Ataeepour M, Farajkhah N K (2013) Quantitative seismic pre-stack analyses of potential gas-hydrate resources in the Makran Accretionary Prism, offshore Iran, Marine and Petroleum Geology, 48: 160-170.
20. Ecker C (1998) Seismic characterization of methane hydrate structure, Ph.D. Thesis, Stanford University.
21. Yari H, Nabi Bidhendi M, Keshavarz Faraj Khah N, Heidari R (2019) Development of hybrid models of rock physics based on effective medium theory, SE Iran, 3th National Iranian Conference on Gas Hydrate, University of Science and Technology of Mazandaran, Iran, 1-10.
22. Sloan E D (1998) Clathrate hydrate of natural gases, Marcel Dekker, Inc, New York.

Archive of SID.ir